Indoor Localization With a Single Wi-Fi Access Point Based on OFDM-MIMO

Shuai Han ⬤, *Senior Member, IEEE*, Yi Li, Weixiao Meng, *Senior Member, IEEE*, Cheng Li, *Senior Member, IEEE*, Tianqi Liu, and Yanbo Zhang

Abstract—In this paper, we propose S-Phaser, an indoor localization system that uses a single Wi-Fi access point (AP) to locate terminals. Compared to traditional indoor localization systems based on the fingerprint positioning technology, S-Phaser does not need to deploy a large number of APs and has better localization accuracy. S-Phaser utilizes channel state information (CSI) to compute the direct path length between a single AP and terminals, thereby efficiently improving the accuracy in the line-of-sight (LOS) scenario. S-Phaser is still able to get satisfied accuracy in the non-LOS scenario even not as good as in the LOS scenario. Using the feature of multiple channels in 802.11n, we design an interpolation-based algorithm, named as the interpolation elimination method to calibrate signal phases from CSI, and then we use two different algorithms, the Chinese residue theorem and broadband angle ranging, to compute the real distance of the direct path from the calibrated phases. Then, S-Phaser uses a geometric positioning algorithm to determine the user's location. To verify the practicability of the proposed S-Phaser, we set up a localization system in an actual environment. S-Phaser can improve the median localization error to 1.5 m with a single Wi-Fi AP.

Index Terms—Channel state information (CSI), indoor localization, single access point.

I. INTRODUCTION

WITH the rapid development of mobile Internet and wireless communication technology, location-based services have become a part of people's lives and provide great convenience in traveling, shopping, and dating. Therefore, precise indoor localization technology has attracted considerable attention. Unlike outdoor localization, which has line-of-sight (LOS) transmission paths, indoor localization faces a diverse propagation environment, including the multipath effect, shadowing, and fading [1]. Because indoor areas are smaller than the outdoor areas, it is important for an indoor localization system to achieve high accuracy in practical applications. Some studies have employed Wi-Fi fingerprints to design precise indoor localization systems and have obtained great localization accuracy. A heat-map-based Wi-Fi fingerprint system, named as HMF, was proposed in [2]. HMF utilizes the building layout as an additional input factor and improves the localization accuracy of the traditional system to 1.5 m in median localization error. Another fingerprint system [3] utilized the similarity of access points (APs) to divide the fingerprint into different clusters and uses the weighted K nearest neighbors (WKNN) algorithm to estimate the location of the terminal, and this work states that the accuracy can be improved by 17.14%. There are also some other new fingerprint systems that can improve the localization accuracy to the decimeter level [4]–[7]. Fingerprint-based indoor localization systems can achieve high accuracy through deploying converged systems or upgrading classification algorithms, but such systems need to deploy many APs that can be scanned by a user's terminal in every location or deploy other auxiliary sensors to assist in establishing a fingerprint. Consequently, the localization accuracy of the fingerprint system is gradually increased, but the complexity of the deployment is high.

Because of the rapid changes in indoor environments, such as shop renovations or mall upgrades, a localization system with low deployment complexity is very important. Therefore, some indoor localization systems based on a single Wi-Fi AP have been proposed. CUPID [8] utilized channel state information (CSI) to extract the signal strength and the angle of the direct path signal to estimate the angle and distance of a terminal to an AP. CUPID can provide a median localization error of 5 m, which is worse than that of general fingerprint localization systems. SAIL [9] combined CSI and human motion to compute the propagation delay of the direct path, eliminating the multipath effect and yielding accurate distance estimation with a mean error of 2.5 m. Although the above systems reduce the complexity of deployment, their localization accuracy is not sufficient. Chronos [10] is the first decimeter-level indoor localization system. This system is based on a multiple-input multiple-output (MIMO) AP to solve time-of-flight from CSI obtained from multiple frequency channels and determine the terminal position from the distance between each antenna and terminal. Chronos has great localization accuracy and low deployment complexity, but its algorithm requires the single AP to collect data over multiple frequency channels, which results in a large positioning delay, and the localization accuracy depends on the number of monitored channels. Thus, if the indoor

This article has been accepted for inclusion in a future issue of this journal. Content is final as presented, with the exception of pagination.

2   IEEE SYSTEMS JOURNAL

environment cannot provide more free channels for Chronos, then the localization accuracy of the system will be reduced.

To implement a precise indoor localization system that does not depend on the number of monitored channels, we propose a single AP scheme based on the phase of CSI. The proposed system, named as S-Phaser, works on a single AP and collects CSI on two different channels. The system obtains precise CSI data using a phase-based error elimination algorithm, and then it combines the power and delay of two channels in the time domain to calculate the distance between the AP and the terminal. Finally, the system can immediately obtain the terminal position through the distance by geometrical positioning.

Our main contributions in this paper can be summarized as follows.

1) To the best of our knowledge, we propose the first algorithm, named as the interpolation elimination method (IEM), to obtain a high-accuracy transmission phase and delay by eliminating the linear phase through interpolation. Through the original error elimination algorithm, we can limit the fluctuation of the phase in $\pi/4$.

2) S-Phaser can obtain great localization performance by frequency hopping only in two different channels. To the best of our knowledge, S-Phaser is the first system to obtain a median localization error of 1.5 m without depending on the number of monitored channels. In a previous study, frequency hopping over five bands was the primary solution to overcome multipath effect.

The remainder of this paper is organized as follows. We introduce the preliminary knowledge about CSI and the sources of CSI measurement error in Section II. Section III presents the IEM algorithm for eliminating phase and angle error, and simulation results based on offline data are presented. We then introduce two original transmission distance estimation algorithms, i.e., a time-based algorithm, named as the Chinese residue theorem (CRT) and a power-based algorithm, named as broadband angle ranging (BAR), and we present the simulation results of the two algorithms in Section IV. Section V presents the structure and workflow of the S-Phaser system. Finally, we draw conclusions in Section VI.

II. PRELIMINARIES

A. Theoretical Foundation

Compared with the traditional indoor localization system based on received signal strength indication (RSSI), the system based on CSI performs better [11]. CSI describes a signal's propagating feature from the transmitter to the receiver and represents effects such as scattering, fading, and power decay with distance. CSI has both amplitude and phase information, and it reflects multipath characteristics, thus making it more suitable than RSSI for an indoor localization system.

In a wireless device that uses orthogonal frequency-division multiplexing (OFDM), signals are modulated to orthogonal subcarriers of different frequencies. The receiver receives a superposition of the signals from different orthogonal subcarriers.

TABLE I
NUMBER OF SUBCARRIERS SENT

Bandwidth	N_g	N_s	Subcarriers to be transmitted
20 MHz	1	56	-28,-27,$\cdots$,-2,-1,1,2,$\cdots$,27,28
	2	30	-28,-26,-24,$\cdots$,-2,-1,1,3,5,7,$\cdots$,25,27,28
	4	16	-28,-24,-20,-16,-12,-8,-4,-1,1,5,9,13,17,21,25,28
40 MHz	1	114	-58,-57,$\cdots$,-3,-2,2,3,$\cdots$,57,58
	2	58	-58,-56,-54,$\cdots$,-4,-2,2,4,$\cdots$,54,56,58
	4	30	-58,-54,-50,$\cdots$,-6,-2,2,6,$\cdots$,50,54,58

The above process can be expressed as [12]

$$Y(f) = H(f)X(f) \tag{1}$$

where f is the transmission frequency, $X(f)$ and $Y(f)$ are the spectra of the transmitted signal and received signal, respectively, and $H(f)$ is the channel frequency response (CFR) at each subcarrier. CFR can be calculated by CSI, which can be obtained from commodity Wi-Fi network interface cards (NICs), such as Intel 5300 by CSI-Tools [13]. Through the data packets received from the network cards, we can obtain a complex vector, where each element in the vector represents the CSI of a subcarrier.

The conversion from the CSI to the CFR is [14]

$$\text{CFR} = \text{CSI} \times \sqrt{\text{SNR}} = \text{CSI} \times \sqrt{\frac{P_{RSS} \cdot P_{CSI}}{\sum n}} \tag{2}$$

where n is the power of noise, which can be obtained from network cards by CSI-Tools, SNR is the signal-to-noise ratio of the antennas on network cards, P_{RSS} is the power to describe the received signal strength, and P_{CSI} is the received power of CSI.

Intel 5300 NICs support the 802.11n protocol with three antennas and cover the 2.4 and 5 GHz bands. In the transceiver, we can choose a 20-MHz bandwidth and a 40-MHz bandwidth to send data packets. A different bandwidth means a different number of subcarriers. The total number of subcarriers and the carriers sent in different bandwidths are shown in Table I [15].

In Table I, N_g is the number of groups in a method that reduces the size of the CSI data by reporting only one value for each group of N_g adjacent subcarriers. N_s is the number of subcarriers.

After the calculation of (2), CSI can be changed to a linear unit CFR that is given in [12]

$$H_{f_k} = \sum_{p=1}^{L} a_p e^{-j2\pi f_k \tau_p} \tag{3}$$

where L is the number of multipaths, f_k is the carrier frequency, a_p is the amplitude of the pth path, and τ_p is the transmission delay of the pth path.

Fig. 1 shows the CFR of 50 packets collected offline at the same location. The bandwidth is 20 MHz, and N_s is 30.

In addition to the frequency-domain information CFR, we can obtain time-domain information and power information from CSI. Through the inverse discrete Fourier transform (IDFT), we can obtain the time-domain information, which is called channel
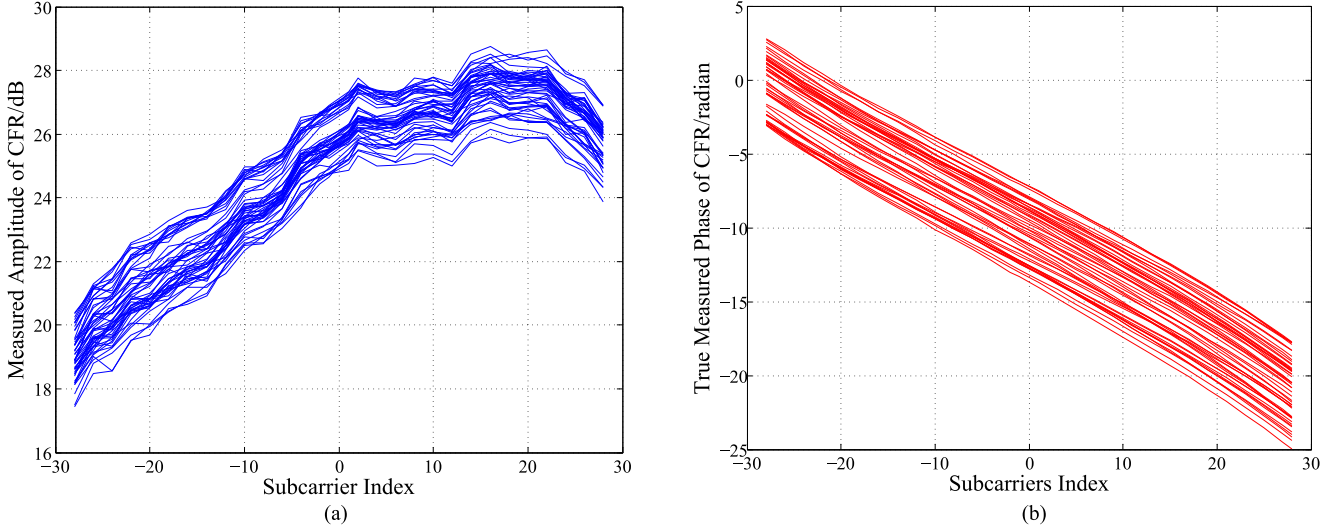
This article has been accepted for inclusion in a future issue of this journal. Content is final as presented, with the exception of pagination.

HAN *et al.*: INDOOR LOCALIZATION WITH A SINGLE WI-FI ACCESS POINT BASED ON OFDM-MIMO

3

Fig. 1.   CFR. (a) Amplitude information of the CFR in dB. (b) Phase information extended from the raw phase information between $-\pi$ and π.
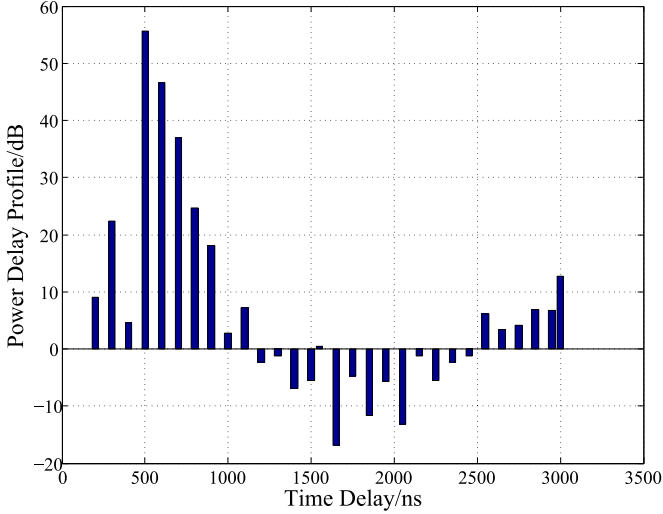

Fig. 2.   Power delay profile.

Fig. 3.   Flow of signal processing in 802.11.

impulse response (CIR) [12]

$$h(\tau) = \sum_{p=1}^{L} a_p e^{-j\theta_p} \delta(\tau - \tau_p). \tag{4}$$

The power delay profile (PDP) is the distribution of the signal power at different delays. The PDP can be calculated from CIR as [9]

$$p(\tau) = E[|h(t,\tau)|^2]. \tag{5}$$

Fig. 2 shows the PDP in dB. As shown, the maximum power does not appear in the first component. It is generally assumed that the first arriving peak is the received power of the direct path. If the first peak is the highest power peak, then it indicates that there is a LOS path between the transmitter and the receiver, and vice versa.
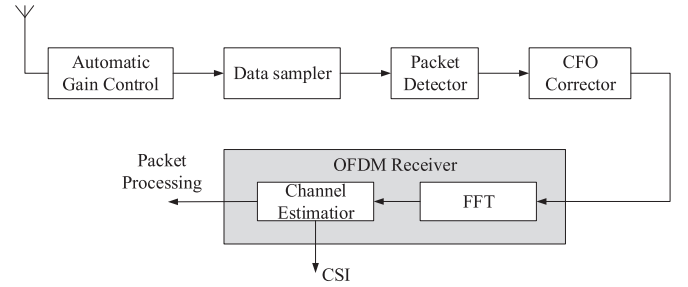
B. Phase Error

Fig. 3 shows the process of the receiver calculating the CSI from received packets [16]. The central frequencies for a pair of transmissions are rarely synchronized perfectly. Thus, the carrier frequency offset (CFO) needs to be compensated by the CFO corrector of the receiver, but due to hardware imperfections, the compensation is generally incomplete. Residual CFO leads to a time-varying phase offset across subcarriers. Packet detection delay, including energy detection delay and correlation detection delay, occurs in digital processing and analog-to-digital conversion (ADC) sampling. The sampling frequencies of the transmitter and the receiver, which have an offset due to nonsynchronized clocks, can cause a time shift of the received signal after ADC [17].

Fortunately, we can analyze the phase data from CSI. There is a linear relationship between the received phase and the subcarrier index. Previous studies [18] have reported that the measured CSI phases are distorted with various phase offset errors. The measured phase $\phi_{i,k}$ at the kth subcarrier in the frequency channel i can be expressed as

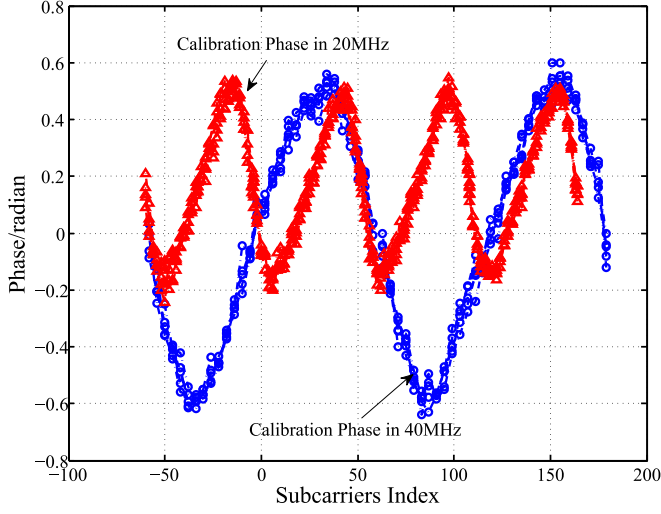$$\phi_{i,k} = \theta_{i,k} - \frac{2\pi K_k \delta_i}{N} + \beta_i + Z \tag{6}$$

Fig. 4.   Calibration phase by traditional elimination method of 20 and 40 MHz.

Fig. 5.   Calibration phase after IEM algorithm and traditional elimination method.

where K_k is the subcarrier index, conforming to $f_{i,k} = f_{i,0} + K_k \cdot \Delta f$, $f_{i,0}$ is the center frequency of band i, Δf is the carrier frequency interval, whose ranges refer to Table I, $\theta_{i,k}$ denotes the true phase without phase offset, δ_i is the equivalent timing offset at the receiver, including time shift of packet detection delay and sampling frequency offset, N is the fast Fourier transform size, β_i is the equivalent phase offset at the receiver, and Z is the nonlinear phase offset because of the noise.

III. ELIMINATION OF PHASE ERROR AND ANGLE ERROR

A. Phase Error Elimination

Based on the phase error model of (6), many error elimination algorithms have been proposed. A current error elimination method is presented in [19] and [20]. The key idea is to eliminate δ and β by considering the phase across the entire frequency band. Assume that the estimated phase is $\widetilde{\phi}_{i,k}$, and it can be defined as

$$\widetilde{\phi}_{i,k} = \phi_{i,k} - K_k a - b \tag{7}$$

where $a = (\phi_{i,w} - \phi_{i,1})/(K_w - K_1)$ and $b = \sum_{j=1}^{w} \phi_{i,j}/w$. The phase is obtained by eliminating the linear phase method as

$$\widetilde{\phi}_{i,k} = \theta_{i,k} - \frac{\theta_{i,w} - \theta_{i,1}}{K_w - K_1} K_k - \frac{\sum_{j=1}^{w} \theta_{i,j}}{w} + \frac{2\pi\delta_i}{Nw} \sum_{j=1}^{w} K_j. \tag{8}$$

The IEEE 802.11n protocol supports two-band mode, namely, 20 MHz HT20 mode and 40 MHz HT40 mode. We use the network card in two different work modes to collect CSI, and then we utilize the error cancellation method in (7) to obtain the calibration phase, which is shown in Fig. 4.

In Fig. 4, we collect the CSI with four consecutive 20 MHz channels at the same static location. The relation between subcarrier bandwidths of 20 and 40 MHz is presented in [15]. Note that the upper part of the 40 MHz transmission has a phase offset of 90°. As shown in Fig. 4, the calibration phases in the two transmission modes are not the same. There are two
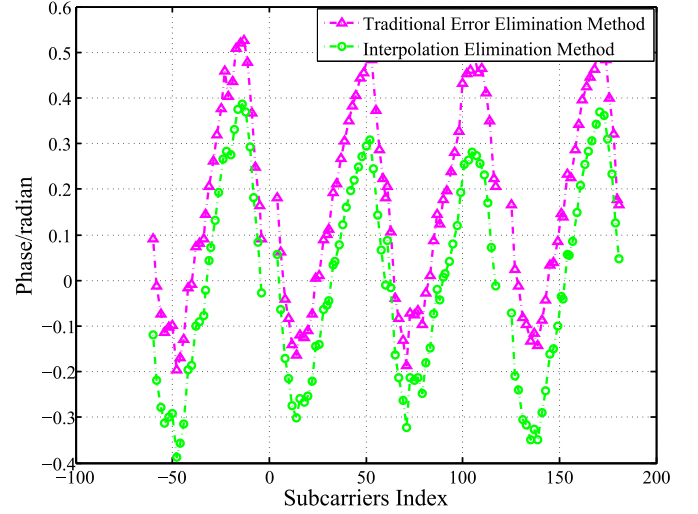
reasons for this difference. First, for the HT20 transmission mode, the CSI subcarriers collected from Intel 5300 NICs are asymmetric, which means that the element $\sum_{j=1}^{w} K_j$ in (8) is not equal to zero. Thus, this leads to a calculation phase error in the HT20 mode. Second, the HT40 mode can be considered as two adjacent 20-MHz channels bundled together for information transmission, and the center frequency is the median value of the two bound channels. Therefore, when the error is eliminated, the subcarriers of the two bound channels should be separated to execute error calibration.

For all the above issues, we propose an algorithm called IEM to eliminate the error using interpolation. The subcarrier below the center frequency is constant, and then we invert the constant index value to obtain a completely symmetrical subcarrier index. In our system, the subcarrier index after the overturn is

$$\widetilde{k} = -28, -26, \ldots, -2, -1, 1, 2, \ldots, 26, 28. \tag{9}$$

Using the new subcarrier index to calculate the phase, we can eliminate the phase error caused by subcarrier index asymmetry. At the same time, extending the a in (7) will yield

$$a = \frac{\theta_{i,w} - \theta_{i,1}}{K_w - K_1} - \frac{2\pi\delta_i}{N}. \tag{10}$$

The phase error eliminated by the symmetric subcarrier contains an error term

$$\frac{2\pi\delta_i}{N} = \frac{(\phi_{\mathrm{asy}} - \phi_{\mathrm{sy}}) \cdot w}{\sum_{j=1}^{w} K_j} \tag{11}$$

where ϕ_{asy} is the phase obtained under the asymmetric index k and ϕ_{sy} is the phase under symmetric index $\widetilde{k}$. The calibration phase after IEM compared with the raw calibration phase is shown in Fig. 5. The difference between the two phase data is 11.5°.

The calibration phase obtained by the IEM algorithm only has the mean item $\sum_{j=1}^{w} \theta_{i,j}$, which is different from the real phase θ_i. According to [16], we know that for an individual
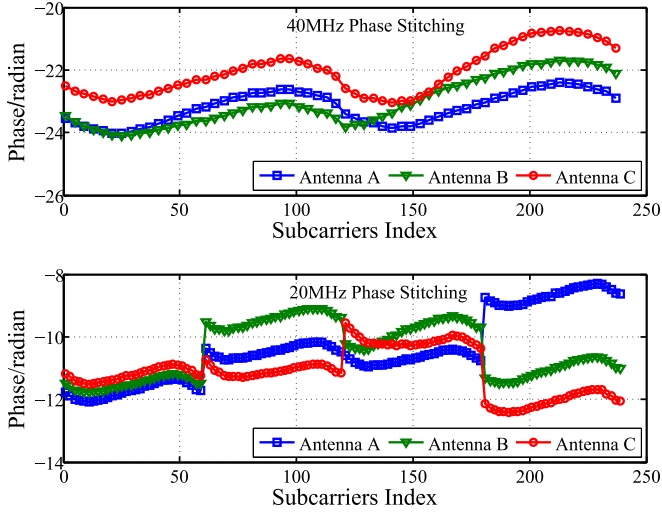
This article has been accepted for inclusion in a future issue of this journal. Content is final as presented, with the exception of pagination.

HAN *et al.*: INDOOR LOCALIZATION WITH A SINGLE WI-FI ACCESS POINT BASED ON OFDM-MIMO 5

Fig. 6. Splicing phase in HT20 and HT40 modes.

Fig. 7. Calibration phase and raw phase in polar coordinates.

Fig. 8. Splicing amplitude in HT20 (20 MHz) and HT40 (40 MHz) modes.

Wi-Fi band, the phase error $\sum_{j=1}^{w} \theta_{i,j}$ has no impact on the derived PDP.

In order to obtain higher temporal resolution, we splice the information of the continuous band. The splicing 20 and 40 MHz correction phases are shown in Fig. 6. As shown, the phase result in 40 MHz is much better than the result in 20 MHz because the 40-MHz frequency band is not overlapping and has a small interference.

B. Angle Error Estimation

As is known, wireless signals arrive at APs from several angles. If we can find the angle of the direct path from a terminal, then it is possible to obtain the location of the terminal by combining the angle of arrival and distance. The core idea is to estimate the angle of arrival using the signal phase received by multiple antennas. The angle of arrival ϑ and the antenna phase difference $\Delta\varphi$ can be expressed as [21]

$$\vartheta = \arcsin\left(\frac{\Delta\varphi}{\pi}\right). \tag{12}$$

We take the calibration phase information obtained by IEM and the raw phase information on polar coordinates, as shown in Fig. 7. The corrected phase is concentrated in a small range, and it can be considered that the highest amplitude is the direct path phase. In Fig. 7, the peak phases before and after IEM algorithm are different, indicating that the error elimination is effective.

In addition to obtaining the angle of the incoming wave and the antenna, the angle information of the direct path can also obtain an effective phase of the direct path. In the obtained phase image, the phase of the subcarrier with the highest power can be regarded as the phase closest to the direct path [22]. The amplitude information of the CSI obtained in the HT20 mode and the HT40 mode is shown in Fig. 8, and the amplitude information of the HT40 mode is more continuous.

With the phase of the direct path, we can obtain the transmission distance of the direct path. We assume that the obtained
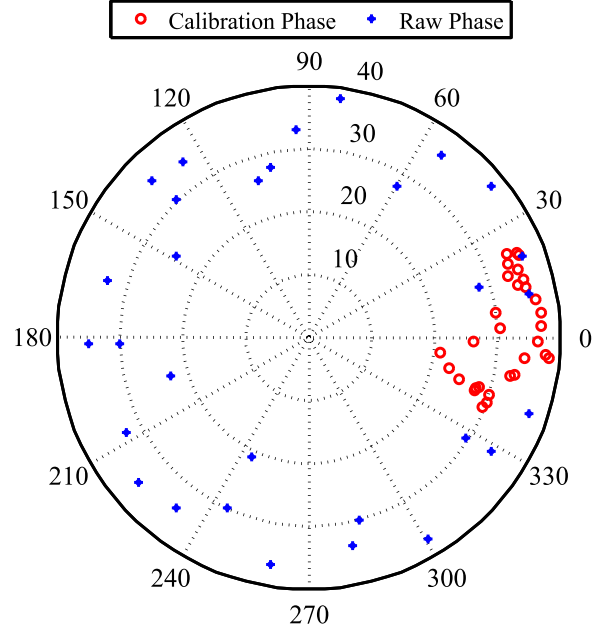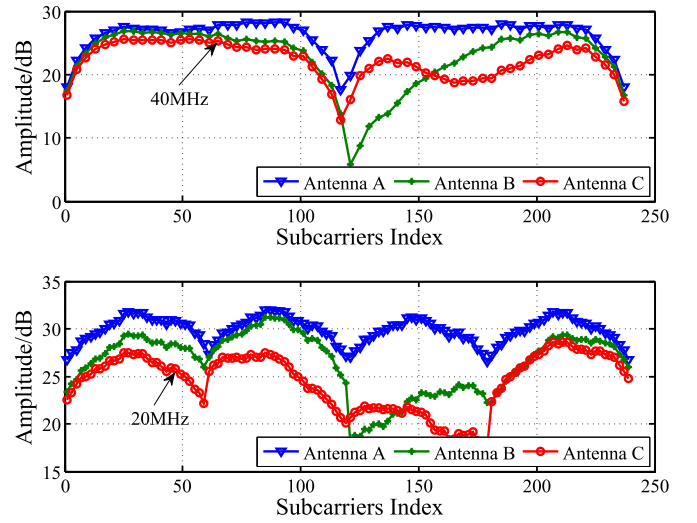
distance is r_i, which can be expressed as

$$r_i = \frac{\widetilde{\phi}_i}{2\pi f_{i,0}} \cdot c \tag{13}$$

where c is the speed of light and $f_{i,0}$ is the center frequency of transmission channel i.

IV. DETERMINATION OF USER LOCATION

A. Distance Estimation Based on CRT

In the previous section, the distance determined from the calibration phase is actually a remainder of the real distance.
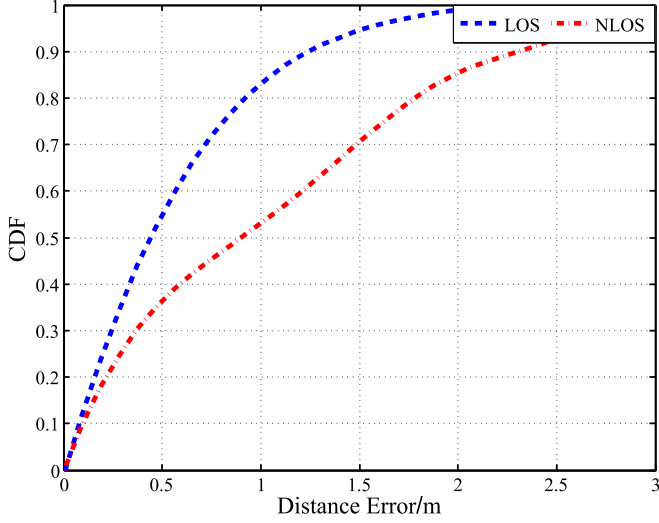
Fig. 9.   CDF of distance error based on CRT.

Fig. 10.   PDP calculated from the splicing CFR.

The true distance d_i is

$$d_i = r_i + m \cdot \lambda_i, \tag{14}$$

where m is a non-negative integer and λ_i is the wavelength of transmission channel i. CRT is an effective method for finding the divisor in the case of known divisors and remainders [23].

The method of splicing the CSI through multiple frequency bands can also be used to solve CRT to obtain more accurate phase information [10]. For the CRT problem (14), when $d_i < M = \prod_{i=1}^{w} \lambda_i$ is satisfied, the real distance can be solved by the following equation:

$$d \equiv \left(\sum_{i=1}^{w} \delta_i r_i \right) (\bmod M) \tag{15}$$

where $\delta_i = Q_i q_i$, $Q_i = M/\lambda_i$, and q_i is the inverse of Q_i. For our system, the shortest transmission wavelength is 5 cm. It is clear that splicing four bands can lead to a calculated distance by CRT that is within 6 m, which is sufficient for the indoor environment.

Through the CSI collected offline, we obtain the remainder of the calibration distance, and we obtain the true distance from the solution of the CRT. The cumulative distribution function (CDF) of distance error is shown in Fig. 9. As shown in Fig. 9, the distance data of the LOS path are more accurate and can reach a distance error limited within 0.5 m of the median localization error.

B. Distance Estimation Based on PDP

Path loss is also a commonly used method to measure the distance, shown as [24]

$$P_R = P_0 - 10\gamma \log(d) \tag{16}$$

where P_R is the received energy at the receiver, P_0 is the received energy at a distance of 1 m from the transmitter, d is the distance
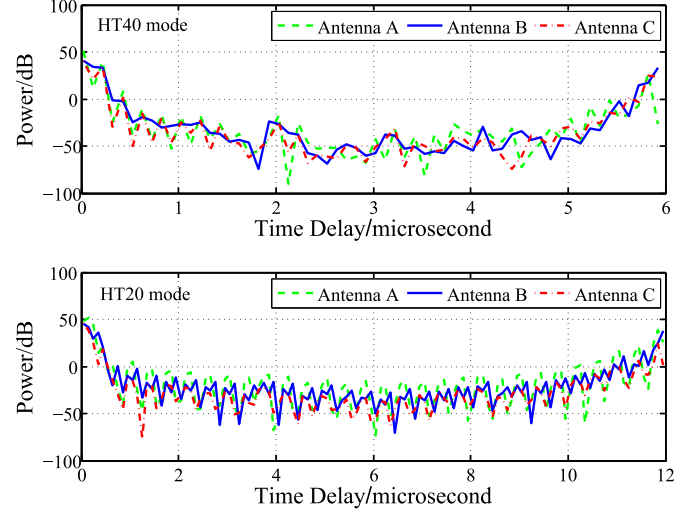
between the transmitter and the receiver in meters, and γ is the path loss exponent.

By frequency hopping, we can obtain the CFR on multiple frequency bands. By combining these bands and using IDFT, we can obtain a CIR with a higher temporal resolution. The time resolution becomes higher because the bandwidth of the postfrequency information is increased. Through the CIR, we can obtain the power delay distribution according to (5). The PDP obtained in the HT20 and HT40 modes is shown in Fig. 10. The PDP reflects the received signal power at different delay times. The first peak is the power of the direct path, and it is P_R in (16). CUPID [8] provides a method for using the PDP to obtain the real distance, in which it assumes that P_0 is the power value of the highest peak in the PDP and the path loss factor is obtained by preacquisition in the environment. However, this method requires preliminary information collection, and the power estimation is not accurate.

We assume that the phase difference between the signal arrivals of antenna A and antenna B is $\Delta\phi$. The wavelength of the signal is λ. By combining with path loss, we can obtain

$$\begin{cases} d_A - d_B = \left(10^{\frac{P_{R,B} - P_{R,A}}{10\gamma}} - 1 \right) d_B \\ d_A - d_B = \frac{\lambda(\phi_A - \phi_B)}{2\pi} \end{cases} \tag{17}$$

where d_A and d_B are the distances from the transmitter to antenna A and antenna B, respectively. $P_{R,A}$ and $P_{R,B}$ are the received power from antenna A and antenna B in the direct path, respectively. ϕ_A and ϕ_B are the phases received from antenna A and antenna B in the direct path, respectively. In this way, the transmission distance can be obtained by the received phase difference. We call the algorithm for obtaining the distance BAR. The CDFs of distance error of CUPID and BAR are compared in Fig. 11.

As shown, the new method BAR has a better distance accuracy, and it can limit the distance to within 0.6 m of the median localization error. Compared with the CRT algorithm, the BAR algorithm does not rely on the number of hops. The BAR algorithm achieves localization performance similar to that of

TABLE II
COMPARISON WITH OTHER SYSTEMS

|	Accuracy	Features	Advantages	Disadvantages
HMF	1.8m	Heatmap-based fingerprinting	Reducing the dependency of training set size	Building layout necessary
WKNN	1.25m	Dividing fingerprint into clusters	Computational complexity reduced; positioning time improved	Time-consuming
CUPID	5m	Utilizing CSI and human mobility	A single off-the-shelf WI-FI AP	Low accuracy
SAIL	2.3m	Utilizing CSI; Wi-Fi ToF-based ranging and smartphone dead-reckoning	A single commodity AP	Low accuracy
Chronos	Decimeter	CSI from multiple channels; MIMO AP	Computing sub-nanosecond time of flight (ToF) using commodity Wi-Fi radios	Large positioning delay; depending on the number of monitored channels
The proposed method	1.5m	OFDM-MIMO; Single Wi-Fi AP; frequency hopping	Accurate transmission distance; positioning costs reduced	Localization accuracy in NLOS environment decreased
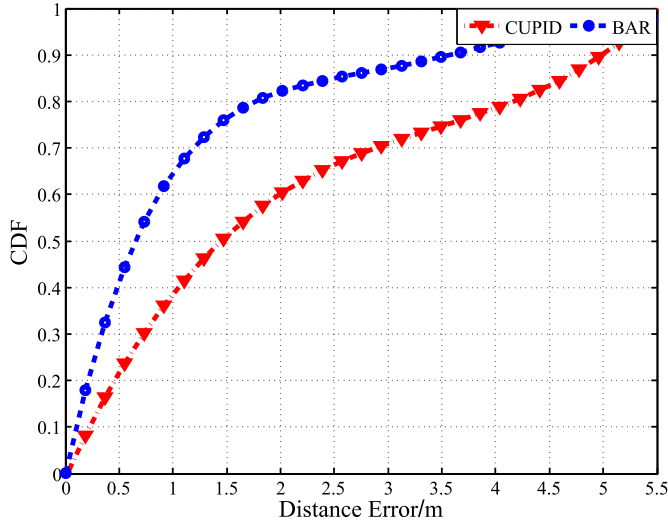
Fig. 11.   CDF of distance error for BAR and CUPID.

Fig. 12.   CDF of localization error for CRT and BAR.

CRT through fewer frequency hops, which means that the BAR algorithm can be applied in more commodity devices.

C. Localization Based on Distance

The most common method for determining the position through the transmission distance is triangulation [25]. When the wireless devices that support OFDM-MIMO have more than three antennas, we can apply triangulation to determine the user's location. Assume that the location coordinate of user is (x, y) and that the location coordinates of the three antennas are (x_1, y_1), (x_2, y_2), and (x_3, y_3). If the distance between the three antennas and the user terminal is known, then the user's coordinate can be solved by the following equation:

$$\begin{cases} temp = (x_1 - x_2) \\ x = (d_1^2 - d_2^2 + d^2)/(2temp) \\ y = (d_1^2 - d_3^2 - x^2 + (x - x_3)^2 + y_3^2)/(2y_3) \end{cases} \quad (18)$$

where d_i is the Euclidean distance between (x_i, y_i) and (x, y).

According to the triangle law, we can evaluate and correct the distance measurement results. If the distance between any two antennas to the user and the distance between the antennas cannot form a triangle, then the distance needs to be corrected.
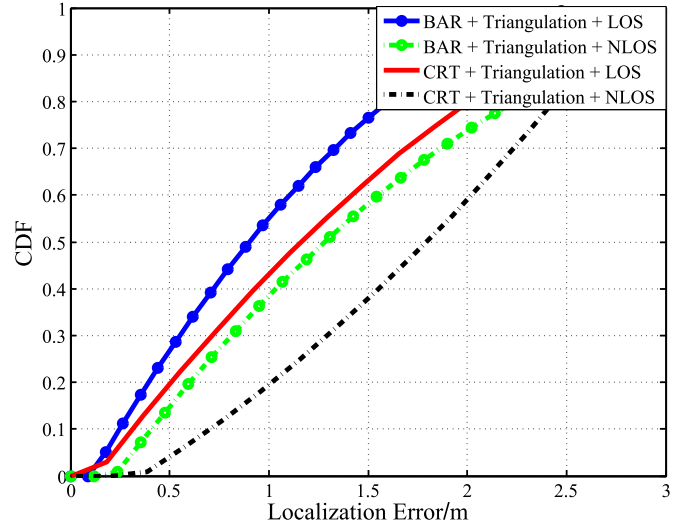
The modified method is to recalculate the error distance using the triangular cosine theorem through the calculated wave direction angle obtained by (12). The selection criterion of the error distance is to find the distance that has the greatest offset from the three calculated distances.

By comparing the real location coordinate with the coordinate calculated by the optimized triangulation, we can obtain the CDF of the localization error, as shown in Fig. 12. As shown in Fig. 12, the localization accuracy for the system using IEM and BAR can achieve 2 m in the case of 60% confidence. The positioning accuracy of the LOS is better than that of non-LOS. Compared to our traditional RSSI-based fingerprint positioning system [26], [27], S-Phaser improves the localization accuracy and reduces the number of APs. Furthermore, some other typical systems features are shown in Table II. Compared to the other systems, the proposed method requires less resources in terms of hardware configuration, computing abilities, and time consumption while can achieve higher accuracy.

V. SETTING UP OF THE ACTUAL LOCALIZATION SYSTEM

To verify that the algorithm is indeed practicable, we constructed a test system for CSI in an actual environment. The
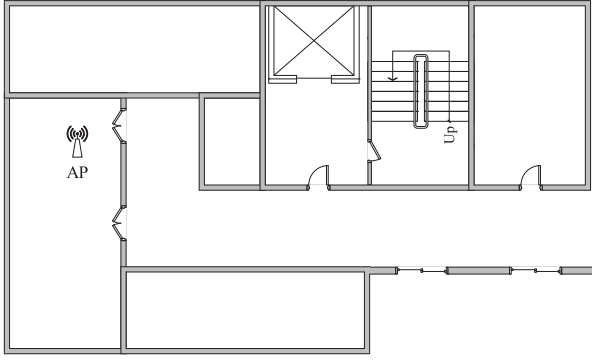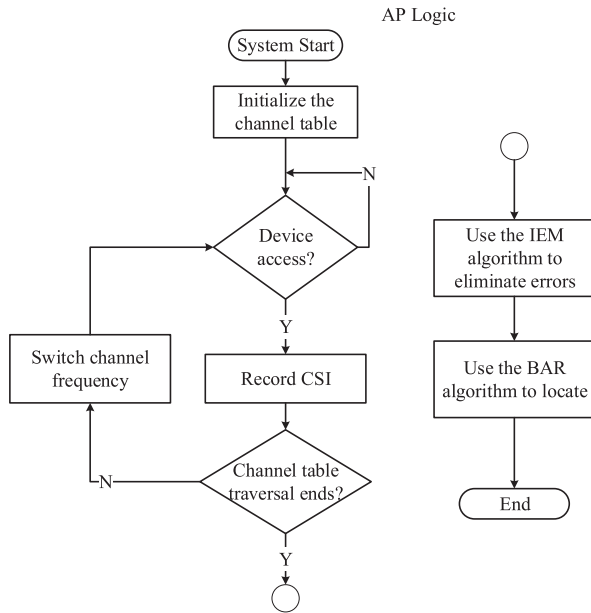
Fig. 13.   Test environment of S-Phaser.

Fig. 14.   Localization system positioning flow.

test environment is shown in Fig. 13. And all the experiment results of the proposed indoor localization are obtained in this test environment.

S-Phaser is a software localization system that runs on an AP. We used a Lenovo ThinkPad T400 notebook running Hostpad software to emulate a single Wi-Fi AP. The notebook computer has preinstalled Intel 5300 NICs. The main program of the localization system is controlled via a shell script, and C language code is used to apply the CSI processing and localization algorithm. The system processing flow is shown in Fig. 14.

S-Phaser starts once user requests are detected. According to the preset channel table, the frequency band is switched, and the data packets are received at the corresponding band. After traversing the channel table, S-Phaser calls the algorithm module to calculate the user's location. After all calculations are complete, the location results are sent to the user.

VI. Conclusion

The single AP localization system is simple to deploy, significantly reducing the positioning costs. Based on basic CSI, this paper gradually eliminates the error related to the transmis-

sion distance. The IEM algorithm, CRT algorithm, and BAR algorithm are proposed to obtain a more accurate transmission distance. We deployed a test system in an actual environment, and we verified the algorithm utilizing the software system S-Phaser, through which we obtained ideal ranging and positioning results.

The test results of the LOS environment are better than the results of the NLOS environment. In the LOS environment, CRT and the BAR-based localization algorithm can achieve 1.5-m localization accuracy with 60% confidence. Compared to the LOS environment, the localization accuracy in the NLOS environment decreased approximately to 40%. The positioning error of the BAR algorithm in the NLOS environment is less than that of the CRT algorithm.

References

[1] K. Chintalapudi, A. Padmanabha Iyer, and V. N. Padmanabhan, "Indoor localization without the pain," in *Proc. 16th Annu. Int. Conf. Mobile Comput. Netw.*, Chicago, IL, USA, Sep. 20–24, 2010, pp. 173–184.

[2] X. Liu, B. Lu, J. Niu, L. Shu, and Y. Chen, "HMF: Heatmap and WiFi fingerprint-based indoor localization with building layout consideration," in *Proc. IEEE Int. Conf. Parallel Distrib. Syst.*, Wuhan, China, Dec. 13–16, 2016, pp. 324–331.

[3] W. Chen, Q. Chang, H. T. Hou, and W. P. Wang, "A novel clustering and KWNN-based strategy for Wi-Fi fingerprint indoor localization," in *Proc. Int. Conf. Comput. Sci. Netw. Technol.*, Harbin, China, Dec. 19–20, 2015, pp. 49–52.

[4] Q. Jiang, Y. Ma, K. Liu, and Z. Dou, "A probabilistic radio map construction scheme for crowdsourcing-based fingerprinting localization," *IEEE Sensors J.*, vol. 16, no. 10, pp. 3764–3774, May 2016.

[5] Y. Shu, Y. Huang, and J. Zhang, "Gradient-based fingerprinting for indoor localization and tracking," *IEEE Trans. Ind. Electron.*, vol. 63, no. 4, pp. 2424–2433, Apr. 2016.

[6] X. Du and K. Yang, "A map-assisted WiFi AP placement algorithm enabling mobile device's indoor positioning," *IEEE Syst. J.*, vol. 11, no. 3, pp. 1467–1475, Sep. 2017.

[7] W. Xu and S. A. Zekavat, "A high-performance measure for non-line-of-sight identification in MIMO-OFDM-based sensor networks," *IEEE Syst. J.*, vol. 8, no. 1, pp. 125–130, Mar. 2014.

[8] S. Sen, J. Lee, K. H. Kim, and P. Congdon, "Avoiding multipath to revive inbuilding WiFi localization," in *Proc. Int. Conf. Mobile Syst., Appl. Services*, Taipei, Taiwan, Jun. 25–28, 2013, pp. 249–262.

[9] A. T. Mariakakis, S. Sen, J. Lee, and K.-H. Kim, "SAIL: Single access point-based indoor localization," in *Proc. 12th Annu. Int. Conf. Mobile Syst., Appl., Services*, Jun. 16–19, 2014, pp. 315–328.

[10] D. V. K. Katabi, "Decimeter-level localization with a single WiFi access point," in *Proc. 13th Usenix Conf. Netw. Syst. Design Implementation*, Mar. 16–18, 2016, pp. 165–178.

[11] Z. Yang, Z. Zhou, and Y. Liu, "From RSSI to CSI: Indoor localization via channel response," *ACM Comput. Surveys*, vol. 46, no. 2, 2013, Art. no. 25.

[12] D. Tse and P. Viswanath, "Fundamentals of wireless communications 12," *ETH Zürich Lecture Script*, vol. 3, no. 5, pp. B6–1–B6–5, 2005.

[13] D. Halperin, W. Hu, A. Sheth, and D. Wetherall, "Tool Release: Gathering 802.11n traces with channel state information," *ACM Sigcomm Comput. Commun. Rev.*, vol. 41, no. 1, 2011, Art. no. 53.

[14] D. Halperin, W. Hu, A. Seth, and D. Wetherall, "Predictable 802.11 packet delivery from wireless channel measurements," in *Proc. ACM SIGCOMM Conf.*, Aug. 30–Sep. 3, 2010, pp. 159–170.

[15] "IEEE 802.11n-2009 Standard," [Online]. Available: http://standards.ieee.org/findstds/standard/802.11n-2009.html, 2009.

[16] Y. Xie, Z. Li, and M. Li, "Precise power delay profiling with commodity WiFi," in *Proc. 21st Annu. Int. Conf. Mobile Comput. Netw.*, Sep. 7–11, 2015, pp. 53–64.

[17] J. Gjengset, J. Xiong, G. McPhillips, and K. Jamieson, "Phaser: Enabling phased array signal processing on commodity wifi access points," in *Proc. 20th Annu. Int. Conf. Mobile Comput. Netw.*, Sep. 7–11, 2014, pp. 153–164.

This article has been accepted for inclusion in a future issue of this journal. Content is final as presented, with the exception of pagination.

HAN *et al.*: INDOOR LOCALIZATION WITH A SINGLE WI-FI ACCESS POINT BASED ON OFDM-MIMO 9

[18] Y. Zhuo, H. Zhu, and H. Xue, "Identifying a new non-linear CSI phase measurement error with commodity WiFi devices," in *Proc. IEEE Int. Conf. Parallel Distrib. Syst.*, Wuhan, China, Dec. 13–16, 2016, pp. 72–79.

[19] X. Wang, L. Gao, and S. Mao, "CSI phase fingerprinting for indoor localization with a deep learning approach," *IEEE Internet Things J.*, vol. 3, no. 6, pp. 1113–1123, Dec. 2016.

[20] C. Wu, Z. Yang, Z. Zhou, and K. Qian, "PhaseU: Real-time LOS identification with WiFi," in *Proc. IEEE Int. Conf. Comput. Commun.*, Kowloon, Hong Kong, Apr.–May 2015, pp. 2038–2046.

[21] R. O. Schmidt, "Multiple emitter location and signal parameter estimation," *IEEE Trans. Antennas Propag.*, vol. AP-34, no. 3, pp. 276–280, Mar. 1986.

[22] J. Xiong and K. Jamieson, "Towards fine-grained radio-based indoor location," in *Proc. 12th Workshop Mobile Comput. Syst. Appl.*, Feb. 28–29, 2012, pp. 13:1–13:6.

[23] E. Weisstein, "Chinese Remainder Theorem," [Online]. Available: http://mathworld.wolfram.com/ChineseRemainderTheorem.html.

[24] S. Han, Z. Gong, W. Meng, and C. Li, "An indoor radio propagation model considering angles for WLAN infrastructures," *Wireless Commun. Mobile Comput.*, vol. 15, no. 16, pp. 2038–2048, 2015.

[25] R. I. Hartley and P. Sturm, "Triangulation," *Comput. Vis. Image Understanding*, vol. 68, no. 2, pp. 146–157, 2001.

[26] W. Meng, Y. He, Z. Deng, and C. Li, "Optimized access points deployment for WLAN indoor positioning system," in *Proc. IEEE Wireless Commun. Netw. Conf.*, Shanghai, China, Apr. 1–4, 2012, pp. 2457–2461.

[27] S. Han, C. Zhao, W. Meng, and C. Li, "Cosine similarity based fingerprinting algorithm in WLAN indoor positioning against device diversity," in *Proc. IEEE Int. Conf. Commun.*, London, U.K., Jun. 8–12, 2015, pp. 2710–2714.

Shuai Han (S'11–M'12–SM'17) received the Graduate degree in communication engineering from Harbin Institute of Technology, Harbin, China. He received the M.E. and Ph.D. degree in information and communication engineering from Harbin Institute of Technology in 2007 and 2011, respectively.

He is currently an Associate Professor with the Department of Electronics and Communication Engineering, Harbin Institute of Technology. His research interests include wireless sensor networks, wireless communications, the global navigation satellite system, and indoor location. Over the academic career, his students and he have contributed in various fields in wireless networks and wireless positioning. His IEEE ICC2017 paper for wireless security was the candidate of best paper. His WiCON2017 paper for full duplex decode-and-forward cooperative relay system was the best paper. As PI, he has four national grants and more than ten industrial grants on wireless networks and positioning. Also, he participated in some major projects on national level in China.

Dr. Han is an Associate Editor of IEEE ACCESS AND JOURNAL OF COMMUNICATIONS AND INFORMATION NETWORKS. He has served as a Co-Chair for technical symposia of international conference ICC 2018, VTC FALL 2016, IWCMC 2017, IWCMC 2016, IWCMC 2015, and WiCON 2017. He has also served as the TPC member for many international conferences, including the IEEE ICC, IEEE GLOBECOM, VTC, IEEE COMNETSAT, and APCC. Also, he is a Senior Member of IEEE Communication Society, Vice Chair of IEEE Harbin ComSoc Chapter, and Vice Chair of IEEE Harbin VTS Chapter. And he completed his Postdoctoral work in 2012 in electrical and computer engineering from Memorial University of Newfoundland in Canada.
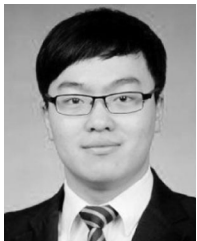
Yi Li received the B.S. and M.S. degrees from Harbin Institute of Technology, Harbin, China, in 2015 and 2017, respectively.

He is currently working with Hangzhou HUAWEI Research Institute, Hangzhou, China. His research interests include sensor network, indoor localization, and cloud computing.

Weixiao Meng (SM'10) received the B.Eng., M.Eng., and Ph.D. degrees from the Harbin Institute of Technology (HIT), Harbin, China, in 1990, 1995, and 2000, respectively.

From 1998 to 1999, he was with NTT DoCoMo on adaptive array antenna and dynamic resource allocation for beyond 3G as a Senior Visiting Researcher. He is currently a Full Professor and the Vice Dean of the School of Electronics and Information Engineering, HIT. He has published 3 books and more than 230 papers on journals and international conferences. His research interests include broadband wireless communications and networking, MIMO, GNSS receiver, and wireless localization technologies.

Dr. Meng is the Chair of IEEE Communications Society Harbin Chapter, a Fellow of the China Institute of Electronics, a Senior Member of the IEEE ComSoc, and the China Institute of Communication. He has been an Editorial Board Member for Wiley's *WCMC Journal* since 2010, an Area Editor for *PHYCOM Journal* since 2014, an editorial board member for IEEE COMMUNICATIONS SURVEYS AND TUTORIALS since 2014, and IEEE WIRELESS COMMUNICATIONS since 2015. He acted as the leading TPC Co-Chair of ChinaCom2011 and ChinaCom2016, leading Services and Applications Track Co-Chair of IEEE WCNC2013, Awards Co-Chair of IEEE ICC2015, and Wireless Networking Symposia Co-Chair of IEEE Globecom2015. In 2005, he was honored provincial excellent returnee and selected into new century excellent talents plan by Ministry of Education, China, in 2008, and the Distinguished Academic Leadership of Harbin.

Cheng Li (SM'07) received the B.Eng. and M.Eng. degrees from Harbin Institute of Technology, Harbin, China, in 1992 and 1995, respectively, and the Ph.D. degree in electrical and computer engineering from Memorial University, St. John's, NL, Canada, in 2004.

He is currently a Full Professor with the Department of Electrical and Computer Engineering, Faculty of Engineering and Applied Science, Memorial University. His research interests include mobile ad hoc and wireless sensor networks, wireless communications and mobile computing, switching and routing, and broadband communication networks.

Dr. Li was a recipient of the Best Paper Award at the 2010 IEEE International Conference on Communications, Cape Town, South Africa, June 2010. He is an Editorial Board Member of Wiley *Wireless Communications and Mobile Computing*, an Associate Editor of Wiley *Security and Communication Networks*, and an Editorial Board Member of *Journal of Networks, International Journal of E-Health and Medical Communications*, and *KSII Transactions on Internet and Information Systems*. He has served as a technical program committee (TPC) co-chair for the ACM MSWIM'14, MSWIM'13, IEEE WiMob'11, and QBSC'10. He has served as a Co-Chair for various technical symposia of many international conferences, including the IEEE GLOBECOM, ICC, WCNC, and IWCMC. He has also served as the TPC member for many international conferences, including the IEEE ICC, GLOBECOM, and WCNC. He is a registered Professional Engineer in Canada and is a member of the IEEE Communication Society, Computer Society, Vehicular Technology Society, and Ocean Engineering Society.

Tianqi Liu received the B.S. degree from the Harbin Institute of Technology, Harbin, China, in 2016. She is currently working toward the M.S. degree with the Harbin Institute of Technology.

Her research interests include NOMA, physical security, and indoor localization.

Yanbo Zhang received the B.S. degree from Harbin Institute of Technology, Harbin, China, in 2017.

He is currently a Research Assistant with Nanyang Technological University, Singapore. His research interest include wireless communication, indoor localization, and sensor network.